P-wave AVAz Modeling: A Haynesville case study

Jon Downton

Hampson-Russell Software, a CGG Company

Summary

For amplitude versus offset (AVO) studies it is common practice to perform forward modelling to understand whether the property of interest is detectable using AVO methods. Using this analogy, this paper argues that modeling the amplitude versus azimuth (AVAz) should be an important part of any AVAz study to detect fracturing. However, this is not the case largely due to the extra complexities of creating and dealing with the anisotropic model needed for these synthetics. This paper demonstrates a practical methodology to create a layered anisotropic model caused by fractures, using linear slip theory and available well log information. Modeling allows the interpreter to determine the magnitude and character of the expected azimuthal response and what azimuthal attributes might best detect the presence of fractures. The utility of this modeling is demonstrated as part of a Haynesville shale gas study.

Introduction

P-wave AVAz modeling can help the interpreter better understand seismic responses related to fractures. In performing such modeling it is easy to become preoccupied with the theoretic complexity associated with anisotropic media and lose sight of the real questions interpreters want answered. For example, for a given reservoir thickness, is it possible to seismically observe the effect of fracturing for a given signal-to-noise ratio? If so, what is the seismic response and what attributes best highlight this response? To try and answer these questions, this paper describes a practical methodology to perform AVAz modeling using well and seismic data for the Haynesville in the Tri-Parish area, Louisiana.

AVAz modeling can be thought of as an extension of AVO modeling. There are many ways to perform forward modeling but for simplicity this paper focuses on convolutional modeling. Typically a 1D layered earth model is assumed for which the interpreter assigns elastic parameters for each layer, often based on well log information. For AVO modeling the reflectivity is calculated at a series of different source-receiver offsets. At each interface between layers, the reflectivity is calculated as a function of offset using the Zoeppritz equation or some approximation. This is done at each interface resulting in a reflectivity series that is then convolved with some source wavelet resulting in an offset dependent synthetic. Wave propagation effects may or may not be considered as part of the modeling.

Extra complexities in performing azimuthal modeling compared to AVO modeling are the major focus of this paper.   First, the interpreter must supply an anisotropic elastic model. Unlike AVO modeling there is not enough information from well logs to uniquely specify the stiffness matrix for anisotropic media. This paper uses linear slip deformation (LSD) theory (Schoenberg, 1980) to construct the anisotropic stiffness matrix due to fractures. The next major source of complexity is how to calculate the azimuthal reflectivity in anisotropic media. Realistic fracture models quickly result in triclinic stiffness matrices necessitating the use of the Zoeppritz equation derived for general anisotropy. Rather than dealing with this complexity, this paper uses a linearized reflectivity approximation derived for general anisotropy due to Pšenčik and Martins (2001). Lastly, the output synthetic must be generated as a function of both offset and azimuth. This also necessitates visualizing the resulting synthetics both as a function of offset and azimuth.

The paper opens with a description of how to generate the anisotropic elastic model used in forward modeling. Linear slip theory is briefly reviewed with the goal of introducing the key concepts and parameters. For simplicity, the discussion is restricted to anisotropy caused by a single set of rotationally invariant vertical fractures and assumes an isotropic background media. Analysis of more complex fracture sets can be found in Collet et al., (2011). It is then shown how a layer based anisotropic elastic model can be constructed using well log information for one of the wells in the study area. Again for simplicity, it is assumed that fracturing is restricted to one particular zone. Having constructed the layered anisotropic model, the calculation of the convolutional synthetic is subsequently discussed.

AVAz modeling is demonstrated on a dataset from the Tri-Parish area on the Louisiana, Texas border. The main target is the Haynesville Formation, which is a black organic-rich shale of Upper Jurassic age. The Haynesville Formation overlies the Smackover Formation and is overlain by the rocks of the Cotton Valley Group. Borehole image logs in the area indicate there is often anisotropy in the Cotton Valley and azimuthal traveltime variations are observed in the seismic below this event. The top of Haynesville is seismically difficult to discern but the large P-wave impedance contrast between the Haynesville and Smackover Formation creates a large reflection which is seismically visible. The azimuthal modeling predicts both the top and base of the Haynesville produce azimuthal anomalies due to fractures. The anomaly associated with the top does not correspond to an event on the stacked section, so it is easy to miss if one is not looking for it. A similar response can be observed in both prestack seismic data and azimuthal attributes.

Methods

The LSD theory models fractures as a perturbation of the compliance of a background rock. The total compliance of the rock **S** is the sum of the background compliance $\mathbf{S}_b$ plus the compliance due to the fractures $\mathbf{S}_f$. The fractures are modeled as an imperfectly bonded interface where the traction is continuous but the displacement might be discontinuous. The displacement discontinuity is linearly related to the traction. For example, the displacement discontinuity normal to the fracture is proportional to the normal stress. This proportionality constant is the normal fracture compliance B_N. In the case of rotationally invariant fractures the tangential fracture compliance B_T may be defined in a similar fashion. This is the case of penny shaped fractures and for vertical fractures normal to the x-axis gives rise to HTI anisotropy (Schoenberg and Sayers, 1995).

The density, P-wave and S-wave velocities from the well logs can be used to calculate the background compliance matrix. Under the above assumptions, the definition of the fractures requires the specification of two fracture parameters. Instead of working with fracture compliances, I choose to parameterize the problem in terms of the normal fracture weakness parameter

$$\delta_N = \frac{MB_N}{1 + MB_N}, \tag{1}$$

and tangential fracture weakness parameter

$$\delta_T = \frac{\mu B_T}{1 + \mu B_T}, \tag{2}$$

where $M = \lambda + 2\mu$, and both λ and μ are Lamé parameters. The fracture weakness parameters are fractional parameters which range from 0 to 1. In all cases when the fracture weaknesses are zero the fracture has no influence on the total compliance.

Stiffness matrix

The stiffness matrix for a single vertical fracture perpendicular to the x-axis in a background isotropic media is (Schoenberg and Douma, 1998)

$$\mathbf{C} = \begin{bmatrix} M(1-\delta_N) & \lambda(1-\delta_N) & \lambda(1-\delta_N) & 0 & 0 & 0 \\ \lambda(1-\delta_N) & M(1-\chi^2\delta_N) & \lambda(1-\chi\delta_N) & 0 & 0 & 0 \\ \lambda(1-\delta_N) & \lambda(1-\chi\delta_N) & M(1-\chi^2\delta_N) & 0 & 0 & 0 \\ 0 & 0 & 0 & \mu & 0 & 0 \\ 0 & 0 & 0 & 0 & \mu(1-\delta_T) & 0 \\ 0 & 0 & 0 & 0 & 0 & \mu(1-\delta_T) \end{bmatrix}, \quad (3)$$

where $\chi = 1-2g$ and g is the square of the S-wave velocity, β, to P-wave velocity, α, ratio of the background isotropic rock. Equation (3) may be used to calculate the stiffness matrix for each layer. This fracture stiffness matrix can be rotated to the fracture strike using a Bond rotation (Winterstein, 1990). For non-fractured layers the normal and tangential weaknesses are zero and the stiffness matrix (equation 3) reduces to its isotropic form. The density, P-wave and S-wave velocity logs can then be used to construct the stiffness matrix.

For fractured media the calculation of the stiffness matrix is a little more complex. In this case the fracture weakness parameters must be specified prior to the calculation. If sonic scanner data is available then Thomsen's γ (Thomsen, 1986) can be calculated from the fast and slow S-wave velocities. The tangential fracture weakness is then calculated from Thomsen's γ using

$$\delta_T = -2\gamma. \quad (4)$$

If borehole image logs are not availble a reasonable value of γ or δ_T can be chosen.

More problematic is the calculation of the normal fracture weakness parameter. There is no logging tool which gives us information about this parameter so we must resort to published values from other sources. Verdon and Wüstefeld (2013) performed a literature review on published values of B_N/B_T. The ratio ranges from 0 to 2 with a median value of 0.65. In performing the modeling it is good practice to experiment with a range of values, though not necessarily equal to 2. Often in practice the upper limit is much smaller than 2, as higher values can lead to nonphysical values of the normal fracture weakness parameter (i.e δ_N >1). The B_N/B_T ratio is thought to convey information about the fluid within the fracture with smaller ratios corresponding to more incompressible fluids (Bakulin et al, 2000).

The modeling shown in this paper uses a B_N/B_T ratio of 0.65. The normal weakness is calculated in the following manner. First, M and μ must be calculated from density, P-wave and S-wave velocity logs. This is straightforward if one assumes the logs represent background velocities. Knowing these parameters and the tangential weakness it is then possible to calculate the tangential compliance using equation (2). Then the normal compliance is calculated from the tangential compliance using the B_N/B_T ratio. Lastly, the normal fracture weakness is calculated using equation (1).

P-wave and S-wave velocity logs can either be interpreted as vertical velocities or background velocities depending on whether the fractures are pre-existing or are being created as part of the modeling exercise. In the latter case, logged P-wave and S-wave velocities correspond to the background velocities and the calculation of stiffness matrix (equation 3) is straightforward. However, if the fractures are pre-existing, then the logged P-wave and S-wave velocities are vertical velocities corresponding to the C_{33} and C_{44} stiffness terms in equation (3). In this case the δ_N, δ_T, M and μ must be solved as a set of nonlinear equations.

Anisotropic elastic layered model

No sonic image logs exist in these data, so a value of -0.1 was chosen for γ over the reservoir interval from 12306 to 12634 ft. This implies 10% S-wave anisotropy and is a starting guess which can be increased or decreased. The B_N/B_T ratio was chosen using the median value of 0.65 resulting in the normal and tangential fracture weakness curves shown in Figure 1. Rather than displaying the stiffness curves it is more intuitive to display the anisotropy in terms of Thomsen parameters. These can be calculated directly from the weakness parameters following Bakulin et al. (2000).

Different poststack attributes can be calculated from the well curves. The zero offset synthetic is calculated from the P-wave impedance log and convolved with the same wavelet as the prestack modeling. The zero offset synthetic shows there is a strong reflector at the base of the Haynesville but essentially no reflection at the top. In a similar fashion, the azimuthal anisotropic gradient (Rüger, 2002) attribute

$$B_{ani} = \frac{1}{2}\left[\Delta\delta^{(V)} - 8\left(\frac{\beta}{\alpha}\right)^2 \Delta\gamma^{(V)} \right] \tag{5}$$

can be calculated from the Thomsen paramters. Figure 1 shows the anisotropic gradient calculated for each interface and then convolved with the same source wavelet as used by the zero offset synthetic. The anisotropic gradient indicates where we might expect to see azimuthal variations. This display indicates that the top of reservoir shows the largest azimuthal variation but unfortunately does not correpsond to any easily picked event on the stacked section. The base is easier to pick and still shows an azimuthal anomaly so that will become our focus. Additional poststack azimuthal attributes such as azimuthal FCs (Downton et al., 2011) can be calculated but are not discussed here for the sake of brevity.
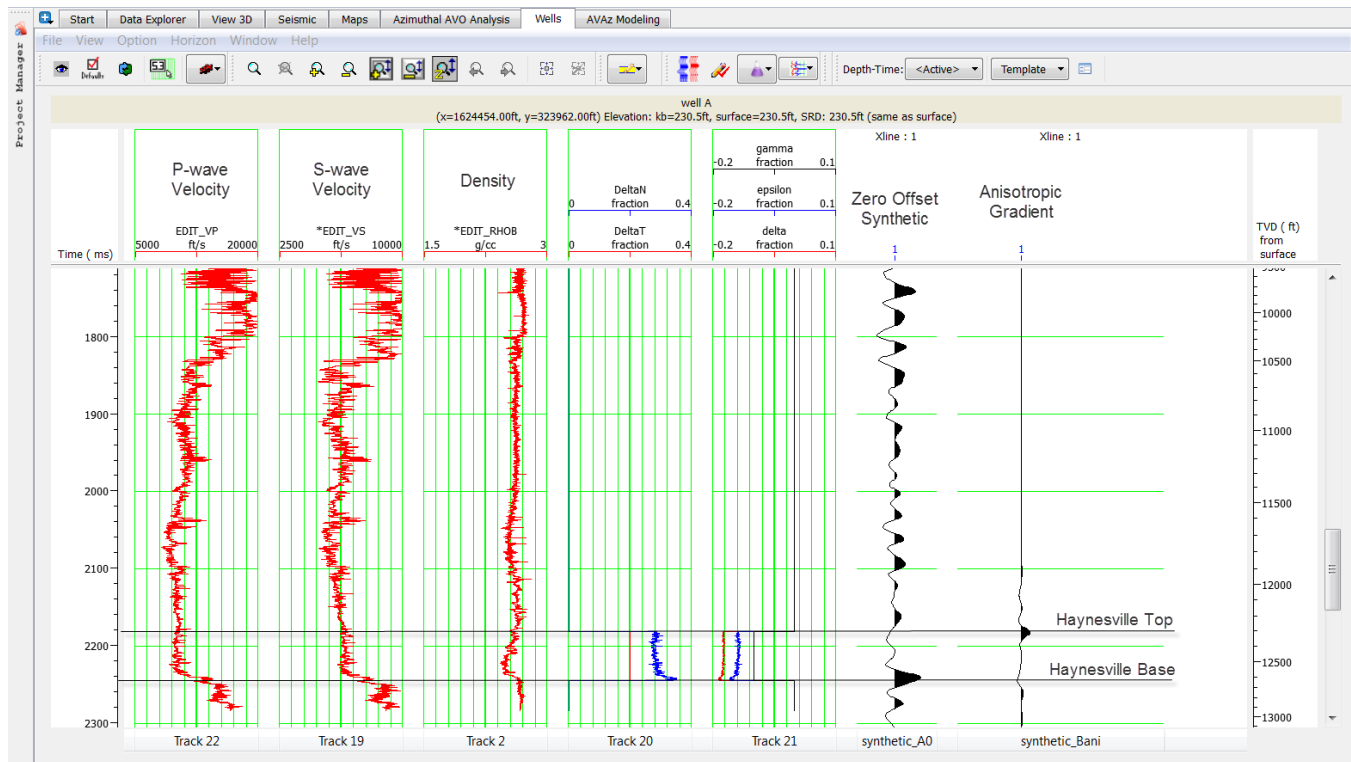

Figure 1: Input elastic model input into the modeling. The Anisotropic Gradient attribute indicates where the azimuthal amplitude variations will be the largest. Note the large variation at the top of the Haynesville does not correspond to a large reflector on the zero offset intercept. The reflector at the base of Haynesville shows both a large reflection and azimuthal variation.

Synthetic model

Having constructed the layered anisotropic model it is now possible to perform the convolutional modeling. In order to do this some output geometry must be specified. For this particular data set the seismic was migrated using an azimuthally sectored migration. Essentially the data was sorted into 6 azimuth sectors over 180 degrees and then each sector was migrated. The modeling was output to a similar geometry.
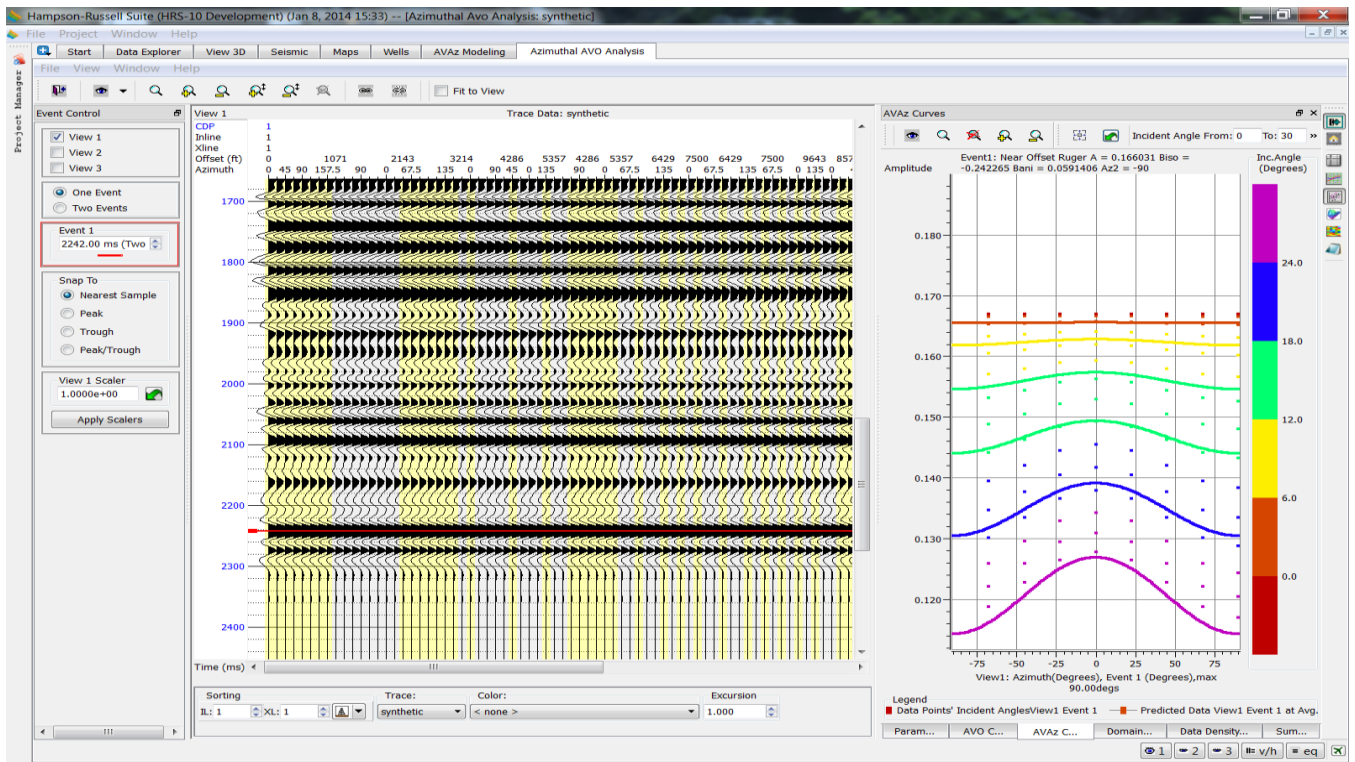
Figure 2: Amplitude versus azimuth analysis of the synthetic data at the base of Haynesville at 2242 ms. The color curves show the amplitude versus azimuth model based on the near-offset Rüger equation at the angle of incidence indicated by the legend. The actual data is shown in the background.
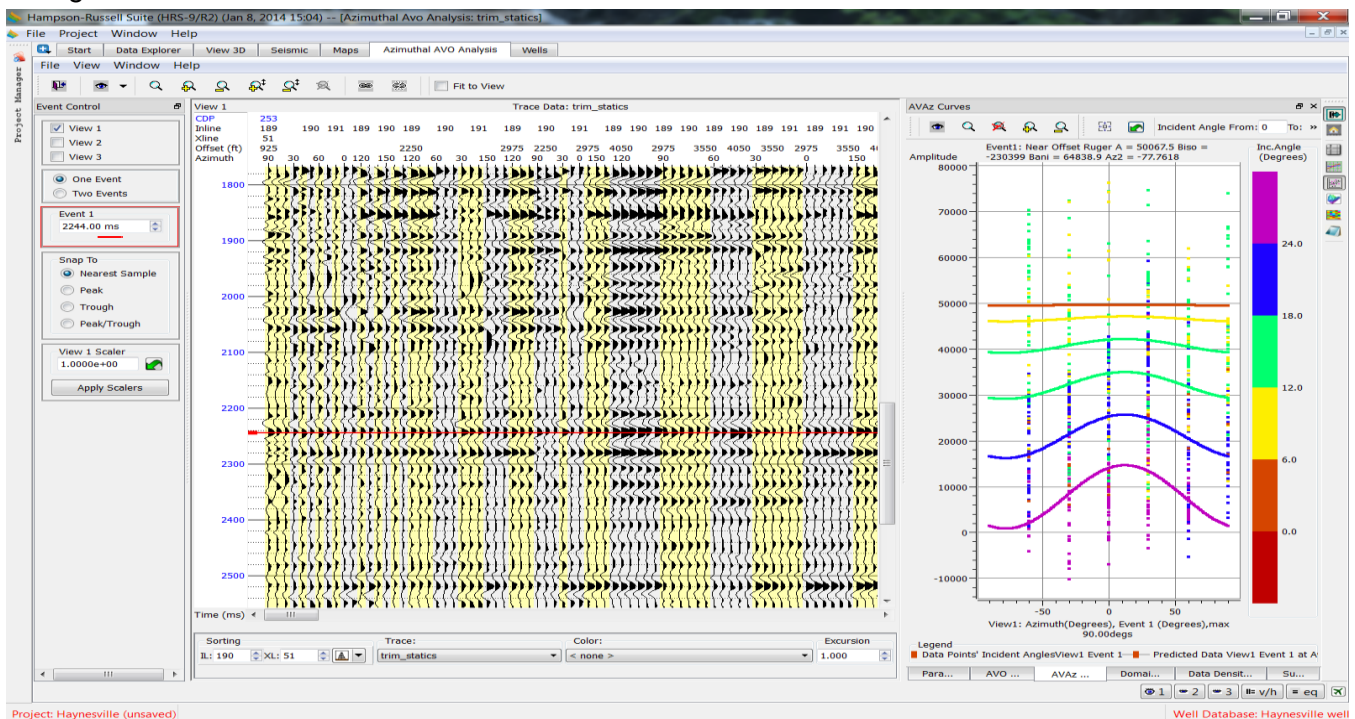

Figure 3: Amplitude versus azimuth analysis of the real data at the base of Haynesville at 2244 ms. The color curves show the amplitude versus azimuth model based on the near-offset Rüger equation at the angle of incidence indicated by the legend. The actual data is shown in the background.

For each interface the reflectivity is calculated as a function of offset and azimuth generating a reflectivity series. The actual reflectivity calculation may be performed by an anisotropic version of the Zoeppritz equation (Schoenberg and Protázio, 1992) or an approximation such as Pšenčik and Martins (2001). The reflectivity series is then convolved with a source wavelet. In this particular case the source wavelet was calculated based on an average of autocorrelations calculated from the seismic volume.

The results of this modeling are shown in Figure 2. The synthetic seismic data is shown as Common Offset Common Azimuth (COCA) gather on the left hand side of the figure. The right side of the figure shows amplitude versus azimuth at the base of Haynesville (red marker at 2242 ms on the seismic). The data is shown as points with the best fit model shown as curves superimposed on top. The model is based on the near-offset Rüger equation and displayed at user specified intervals. The synthetic clearly shows an AVAz anomaly at the base of Haynesville.

The seismic data at the well location (Figure 3) shows a similar AVAz response as the synthetic. Both Figure 2 and Figure 3 show the analysis at the base of Haynesville since it is easier to see, but there is also a an azimuthal response at the top of reservoir.

Discussion

For brevity this paper has generated one synthetic based on a single B_N/B_T ratio. In actual modeling studies it is important to vary the B_N/B_T ratio, because this can change the magnitude of the anisotropic gradient; there exist certain combinations of fracture weaknesses and Vs/Vp ratios for which the anisotropic gradient becomes zero, even in the presence of fractures. Another issue worth studying is the relative contribution of the mid and far offset azimuthal terms. At certain angles of incidence, the two can cancel each other out, annihilating the azimuthal response. In such cases there might exist a stronger AVAz response at nearer angles (i.e. 20 degrees) than larger angles (i.e. 30 degrees). This is easily studied by generating some of the azimuthal FC attributes. Other factors worth studying are the effect of dip (Downton, 2013), the influence of VTI Background media, the effect of pore fluids using the anisotropic Gassmann equation, or added complexity due to multiple fractures.

Conclusions

This paper demonstrates a practical methodology to perform azimuthal modeling and, in particular, how to construct the layered anisotropic model due to fractures. The generation and display of poststack attributes such as the anisotropic gradient or the 2nd azimuthal FC can help the interpreter identify key reflectors where there should be azimuthal variations. This can help guide the interactive AVAz analysis of the synthetic and real data. The example demonstrates that it is possible to model an AVAz response due to fractures, similar to what is seen in the real seismic data.

Acknowledgements

References

Bakulin, A., V. Grechka, and I. Tsvankin, 2000, Estimation of fracture parameters from reflection seismic data—Part I: HTI model due to a single fracture set: Geophysics, **65**, 1788

Collet, O., B. Roure, and J. Downton, 2011, The reflectivity response of multiple fractures and implications for azimuthal AVO inversion; 2011 CSPG CSEG CWLS Convention

Downton, J., B. Roure, and L. Hunt, 2011, Azimuthal Fourier Coefficients: CSEG Recorder, **36**, #10, 22-36

Downton, J, 2013, Characterizing dipping fractures from P-wave Amplitude versus Azimuth studies; 2013 geoConvention

Pšenčik, I. and J. L. Martins, 2001, Properties of weak contrast PP reflection/transmission coefficients for weakly anisotropic elastic media: Studia Geophysica et Geodaetica, **45**, 176-197

Rüger, A., 2002, Reflection coefficients and azimuthal AVO Analysis in anisotropic media: SEG geophysical monograph series number 10: Soc. Expl. Geophys.

Schoenberg, M., 1980, Elastic behaviour across linear slip interfaces: Journal of the Acoustical Society of America, **68**, 1516–1521.

Schoenberg, M. and J. Douma, 1998, Elastic wave propagation in media with parallel fractures and aligned cracks: Geophysical Prospecting, **36**, 571-590.

Schoenberg, M., and C. Sayers, 1995, Seismic anisotropy of fractured rock: Geophysics, **60**, 204–211.

Schoenberg, M., and J. Protázio, 1992, 'Zoeppritz' rationalized and generalized to anisotropy, Journal of Seismic Exploration, **1**, 125-144.

Thomsen, L., 1986, Weak elastic anisotropy: Geophysics 51, p 1954.

Winterstein, D., 1990, Velocity anisotropy terminology for geophysicists: Geophysics, **55**, 1070–1088.

Verdon J.P. and A. Wüstefeld, 2013, Measurement of the normal/tangential fracture compliance ratio (Z_N/Z_T) during hydraulic fracture stimulation using S-wave splitting data: Geophysical Prospecting: Geophysical Prospecting, **61**, 461-477.